Giant Surfactants

International Edition: DOI: 10.1002/anie.201510524
German Edition: DOI: 10.1002/ange.201510524

Molecular-Curvature-Induced Spontaneous Formation of Curved and Concentric Lamellae through Nucleation

Xue-Hui Dong, Bo Ni, Mingjun Huang, Chih-Hao Hsu, Ruobing Bai, Wen-Bin Zhang, An-Chang Shi,* and Stephen Z. D. Cheng**

Abstract: *Spontaneous formation of concentric lamellae was observed in self-assembling giant surfactants consisting of a fluorinated polyhedral oligomeric silsesquioxane (FPOSS) head and flexible polymer tail(s). Owing to the asymmetrical sizes of the head and tail blocks and the rectangular molecular interface, the giant surfactants assumed a truncated-wedge-like molecular shape, which induced morphological curvature during self-assembly, thus resulting in the formation of curved and concentric lamellae. These curved/concentric lamellae were observed in FPOSS-based giant surfactants with different architectures and compositions. The spontaneous curvature formation not only promotes our fundamental understanding of assembly principles, but also provides a promising and efficient approach to the fabrication of a wide range of high-performance devices.*

Concentric ring patterns with nanometer-scale feature sizes are a unique and important geometry that is attractive for many applications, including magnetic and optical memories, transistors, and sensors.[1] The self-assembly of block copolymers provides a versatile platform for nanostructure engineering, as it leads to a variety of ordered phases, including lamellae (LAM), double gyroids (DG), hexagonally packed cylinders (HEX), and body-centered-cubic-packed spheres (BCC), together with other complex morphologies.[2] Concentric rings are in essence a cross-section of either one dimensionally (1D) curved lamellar columns or 2D curved lamellar spheres.[3] The conventional block-copolymer self-assembly process in the bulk typically yields lamellae with flat interfaces containing irregular distortions and/or randomly oriented grains.[4] The formation of curved lamellae with smooth curvatures requires external constraints to impose additional boundary conditions.[5] For example, the restriction of block copolymers in cylindrical nanopores leads to lamella curving and encircling, which releases the packing frustration of confinement.[1c,3,6] The assembly of block copolymers on prepatterned concentric templates is another approach to induce the formation of concentric lamellae.[7] Stringent experimental conditions and complicated processes, however, are usually required, which limit access to and the utilization of this unique structure. It is thus highly desirable to develop methods toward the spontaneous formation of concentric lamellae through the self-assembly of macromolecules.

In a curved bilayer, the outer layer should be in expansion while the inner layer is in compression. For nanostructures self-assembled from block copolymers, the asymmetry of the block size generates imbalanced chain crowdedness at the two sides of the interface. The imbalance can be released through transitions to ordered phases with curved interfaces, such as cylinders, when the thermodynamic phase-stability limit is exceeded. This *phase curvature* is an important characteristic of different ordered structures. On the other hand, a bilayer in the LAM phase is commonly composed of two symmetric monolayers. This symmetry dictates that the spontaneous curvature of a bilayer is zero, and planar lamellae are the equilibrium morphology. Curved or concentric lamellae thus represent intriguing cases in which the curvature of the lamellae, or the *morphological curvature*, is nonzero and the system deviates from intrinsic flat domain interfaces. The spontaneous formation of lamellae with smooth morphological curvatures has not yet been observed in conventional block copolymers, probably because imbalanced chain overcrowding can be relaxed by synergistically adjusting the interfacial area and the chain stretching to maintain a flat interface. For the creation of curved lamellae, a rational molecular design should meet several criteria: I) the morphology should remain in the lamellar phase with certain compositional asymmetry to accommodate internal stress, but this stress should not be sufficient to stimulate phase transitions; II) at least one block should be a nano-object with a fixed shape so that the internal stress cannot be released by expansion or shrinkage of the interfacial area. Moreover, for 1D curvature formation (which is the focus of this study), chain overcrowding should only occur in one direction of the interface and be diminished in the orthogonal direction (otherwise it will result in 2D curvatures).

We recently developed a "clickable" fluorinated polyhedral oligomeric silsesquioxane (FPOSS) building block.[8] It is a shape-persistent molecular nanoparticle with a cylindrical shape.[9] A library of FPOSS-based giant surfactants with either homopolymer or block-copolymer tail(s) have been

[*] Dr. X.-H. Dong, B. Ni, M. Huang, Dr. C.-H. Hsu, R. Bai, Prof. Dr. W.-B. Zhang, Prof. Dr. S. Z. D. Cheng
Department of Polymer Science, University of Akron
Akron, OH 44325 (USA)
E-mail: scheng@uakron.edu
Prof. Dr. W.-B. Zhang
Key Laboratory of Polymer Chemistry and Physics of the Ministry of Education, College of Chemistry and Molecular Engineering, Center for Soft Matter Science and Engineering, Peking University
Beijing 100871 (China)
E-mail: wenbin@pku.edu.cn
Prof. Dr. A.-C. Shi
Department of Physics and Astronomy, McMaster University
Hamilton, Ontario L8S 4M1 (Canada)
E-mail: shi@mcmaster.ca

Supporting information for this article is available on the WWW under http://dx.doi.org/10.1002/anie.201510524.

synthesized and studied.[8–10] These giant surfactants could form lamellae over a broad range of compositions.[9] The polymer tails in the lamellar phase are highly stretched because the FPOSS head cannot provide a sufficient interfacial area for the unperturbed polymer tail(s). Notably, this mismatch in cross-sectional area induced unexpected phase separation between two low-molecular-weight blocks of the tail(s) and led to hierarchical lamellar structures.[9] Herein, we report on the spontaneous formation of curved and concentric lamellae from FPOSS-based giant surfactants. The basic hypothesis is that the asymmetrical block sizes of the head and tail(s) and the rectangular-shaped molecular interface led to a truncated-wedge-like molecular shape of the giant surfactants (Scheme 1c), which generates initial curved

Table 1: Characterization of giant surfactants.

Sample[a]	Phase[b]	d [nm][c]	M_0 [nm^{-1}][d]	M_{max} [nm^{-1}][e]
FPOSS-PS_{36} (**1**)	LAM	10.2	1/93	1/90
FPOSS-PS_{56} (**2**)	LAM	13.2	1/38	1/40
PS_{38}-(FPOSS)-PEO_{45} (**3**)	LAM	12.6	1/85	1/110
PS_{54}-(FPOSS)-PEO_{45} (**4**)	LAM	13.6	1/42	1/60
FPOSS-PS_{48}-b-PEO_{45} (**5**)	LAM	16.8	1/20	1/50

[a] Subscripts represent the degree of polymerization, N. [b] Phase structure. [c] Domain size. [d] Spontaneous curvature, as calculated from Equation (3). [e] Largest accessible curvature, as determined from TEM images.

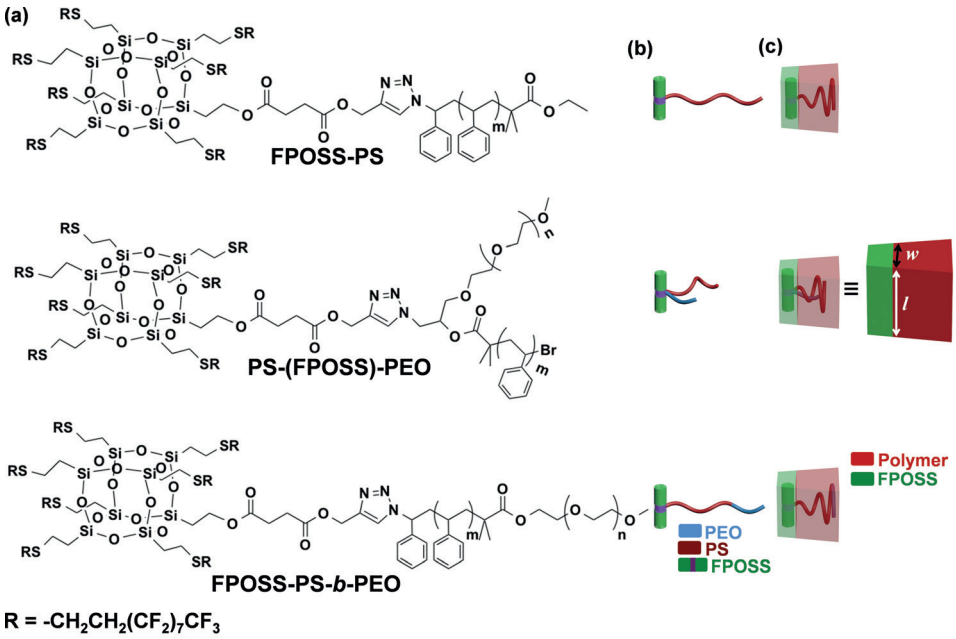

Scheme 1. a) Chemical structures, b) schematic illustrations, and c) molecular shapes of the giant surfactants.

type of curved lamellae with fully closed rings. No specific alignment, for example, shearing or templating, was applied during sample preparation. The overall molecular-packing features of these curved lamellae were the same as for flat lamellae, with alternating FPOSS and polymer domains. Figure 1 shows bright-field (BF) TEM images of the curved lamellae with smooth curvatures. In the simplest case, FPOSS-PS (**1**; Figure 1a; see also Figure S2a), the dark layer is the FPOSS cage domain, whereas the light layer is the PS domain, according to their relative electron densities.[9] For the giant surfactants with block-copolymer tail(s), PS-(FPOSS)-PEO and FPOSS-PS-*b*-PEO, further segregation of the PS and PEO blocks in the polymer domain

nuclei. Further growth from the curved nuclei resulted in the formation of curved or concentric lamellae (Figure 3).

Our experimental observations revealed that curved or concentric lamellae could indeed form spontaneously. To illustrate the generality of our hypothesis, we studied three different types of giant surfactants, specifically, with a polystyrene (PS) tail (FPOSS-PS), with both a PS and a poly(ethylene oxide) (PEO) tail (PS-(FPOSS)-PEO), and with a PS-*b*-PEO block copolymer tail (FPOSS-PS-*b*-PEO; Scheme 1; see also Table S1 in the Supporting Information). All giant surfactants were designed to be in the lamellar-forming region (Table 1; see also Figure S1 in the Supporting Information). Samples were annealed at 110°C for 12 h and characterized by small-angle X-ray scattering (SAXS) and transmission electron microscopy (TEM). Curved lamellae (Figure 1) and concentric lamellae (Figure 2), together with conventional flat lamellae (see Figure S2), coexisted in all three cases. In essence, the concentric lamellae are a particular

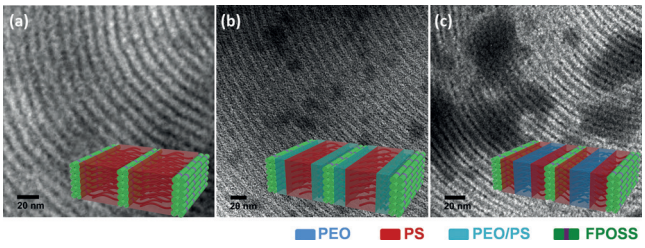

Figure 1. TEM BF images of curved lamellae of a) FPOSS-PS_{56}, b) PS_{38}-(FPOSS)-PEO_{45}, and c) FPOSS-PS_{48}-*b*-PEO_{45}. The corresponding schematic models are included. All samples were stained with RuO_4. Scale bars: 20 nm.

leads to additional lamellar structures. Multilayered nanostructures in the direction along the lamellar normal are observed, with a sequence of FPOSS(gray)/(PEO/PS)(dark)/PS(light)/(PS/PEO)(dark)/FPOSS(gray) for PS-(FPOSS)-

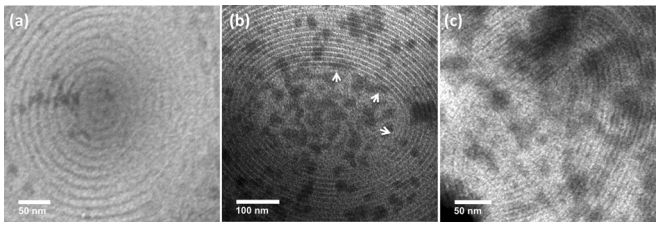

Figure 2. TEM BF images of concentric lamellae of a) FPOSS-PS_{56} (scale bar: 50 nm), b) PS_{38}-(FPOSS)-PEO_{45} (scale bar: 100 nm), and c) FPOSS-PS_{48}-*b*-PEO_{45} (scale bar: 50 nm). All samples were stained with RuO_4.

PEO (**3**; Figures 1b; see also Figure S2b) and FPOSS(gray)/PS(light)/PEO(dark)/PS(light)/FPOSS(gray) for linear FPOSS-PS-*b*-PEO (**5**; Figures 1c; see also Figure S2c; detailed analyses can be found in Ref. [9]). The FPOSS cage domain consists of mesomorphic packed nanocylinders with their long axes perpendicular to the lamellar normal of the polymer layers, and its periodicity is 3.5 nm.[9] The overall domain size varies depending on the length of tails, typically in the range of 10–20 nm, as determined from the SAXS results (Table 1).

The presence of curvature was pervasive in all three cases. The size of the concentric lamellae could extend to tens of micrometers. Most of the concentric rings have an elliptical shape (Figures 2; see also Figures S3 and S4), thus indicating that they are a cross-section of 1D curved lamellar columns rather than 2D curved lamellar spheres; otherwise, a circular pattern would always be observed. Both the flat and curved lamellae have the same domain size, thus indicating no significant packing frustration occurred.[3,6e] Another interesting observation is that the lamellar structure breaks down in the innermost region, probably owing to the excess curvature towards the center. We define a parameter, the *largest accessible curvature* M_{max} ($M_{max} = 1/(2R_{min})$), in which R_{min} is the semi-minor axis of the innermost ellipse (equivalent to the inner radius of the 2D curved lamellar columns), to characterize the size of this disordered center region. Values of M_{max} were estimated from the TEM images (Table 1). There usually exists a distribution of M_{max}, and the largest observed value is adopted as a first approximation. In general, for giant surfactants with the same architecture, M_{max} increases with increasing tail length. For example, **2** has a M_{max} value of 1/40 nm^{-1}, which is larger than that of **1** with a shorter PS tail (1/90 nm^{-1}; see Figure S3). A comparison between **3** and **4** further confirms this trend (see Figure S4).

The morphological curvature originates from the asymmetrical size of head and tail blocks and the rectangular shape of the molecular interface. The FPOSS cage assumes a cylindrical shape with a length of 3.5 nm and a diameter of approximately 1 nm, thus leading to a fixed 2D rectangular molecular interface with a length $l = 3.5$ nm and a width $w =$ 1 nm (Scheme 1c).[9] This interfacial area is smaller than the unperturbed size of polymer tail(s) and thus, chain overcrowding occurs.[9] To alleviate the excluded-volume repulsion, polymer tails are forced to stretch out along the normal of the interface, and also to expand in the perpendicular directions. Owing to the rectangular shape of the interface, the overcrowding along the w direction is much more severe than that in the l direction, thus resulting in a truncated-wedge-like molecular shape (Scheme 1c; see the Supporting Information). Assuming that the assembly process is a nucleation- and growth-controlled process,[11] the truncated-wedge-like molecules could aggregate to form nuclei with a uniform curvature at the initial stage (Figure 3a). Further growth from these sites leads to curved or concentric lamellae. The

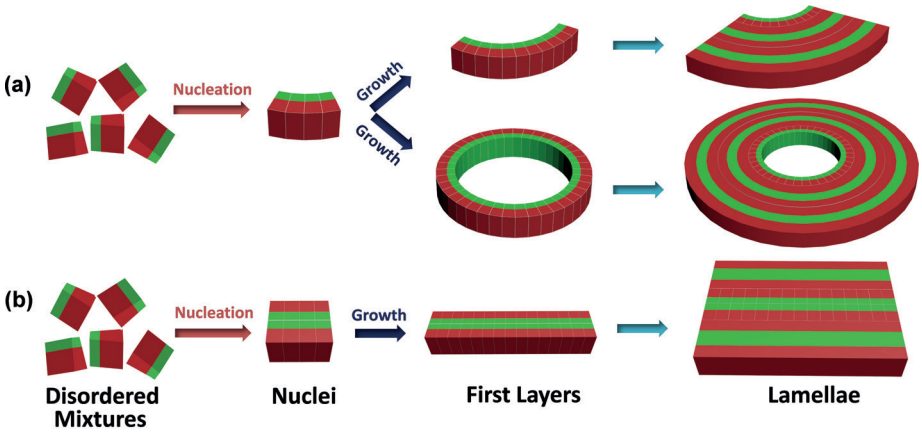

Figure 3. Formation of a) curved/concentric lamellae and b) flat lamellae.

proposed molecular packing indicates that the initial FPOSS domain must be a monolayer (Figure 3a).[3] Indeed, a faint yet clear layer with approximately half the thickness of the FPOSS domain and surrounding PEO domains (the thickness of this combined "dark" domain is approximately 8 nm) is observed in the innermost layer of PS-(FPOSS)-PEO (Figure 2b, arrows). This monolayer is not evident in the other two cases owing to different molecular packing. The FPOSS domain is sandwiched between two PS domains (light layers) in FPOSS-PS and FPOSS-PS-*b*-PEO; therefore, a monolayer of an isolated FPOSS domain (1–2 nm) is difficult to resolve. Additional evidence comes from the initial growth trajectory of the lamellae (see Figure S5). The layer extends in both the radial (along the interfacial normal) and tangential direction (perpendicular to the interfacial normal) of the nuclei, thus resulting in fan-shaped lamellae. There is a sharp phase boundary between the lamellar phase and surrounding disordered phase. Furthermore, the curved/concentric lamellae diminish in the samples quenched from high temperature (above the mesomorphic to isotropic transition temperature of the FPOSS), in which the FPOSS is no longer cylindrical and the truncated-wedge-like molecular shape of the giant surfactant disappears. Flat nuclei also exist with a symmetric, bimolecular packing (see Figure 3b) to form flat lamellae,

although the molecules suffer from chain overcrowding due to the volume mismatch between head and tails.

The initial monolayer nuclei (Figure 3a) can be regarded as a polymer brush system with polymer tails tethered on an FPOSS substrate. A balance between the entropic force of polymer tails to acquire more space and the bending energy arising from deformation of the FPOSS substrate leads to a spontaneous curvature with a free-energy minimum.[12] The total free-energy change per molecule is given by:

$$\Delta F = \Delta F_{el}(R) + \Delta F_{b}(M, G) \quad (1)$$

in which ΔF_{el} is the entropy gain of each polymer tail on a curved surface as compared with a flat surface ($\Delta F_{el} = F_{el,c} - F_{el,f}$); ΔF_b is the bending energy; R, M, and G are the radius, mean curvature, and Gaussian curvature, respectively ($M = 1/(2R)$ and $G = 0$ for cylinders).[13] The F_{el} term can be described using a modified blob model.[12d,14] For polymers on a flat surface, all the blobs have the same diameter, whereas the size of the blobs on a cylindrical surface depends on their distance from the central axis of the cylinder (see Figure S6).[12d] According to the Alexander–de Gennes model,[14a,b] all the free chain ends of tethering polymers are located in the same plane at a distance $h(R)$ from the tethering surface. The height of a tethered tail on a flat surface is $h_0 = N\xi_0 g^{-1} = N b^{1/\nu} \xi_0^{\,1-1/\nu}$, which leads to a free energy of $F_{el,f} = k_B T N (b/\xi_0)^{1/\nu}$, in which b is the monomer size and ξ_0 is the tethering distance between neighboring chains (see the Supporting Information for details).[12d] The free-energy gain for each polymer chain on a cylindrical surface as compared with a flat surface is (see the Supporting Information):[12d]

$$\Delta F_{el} = F_{el,f} f(h_0/2R) \quad (2)$$

in which $f(x) = (1/x)\{[1 + (1+\nu)x/\nu]^{\nu/(1+\nu)} - 1\} - 1$.

On the other hand, bending a flat layer is energetically unfavorable.[12b] The bending energy can be estimated on the basis of the Helfrich model, $\Delta F_b(M, G) = 1/2\kappa S M^2 + \kappa_G S G$, in which κ is the mean bending modulus and κ_G is the Gaussian bending modulus.[13] The spontaneous curvature, M_0, can be obtained by minimizing ΔF with respect to M [Eq. (1)]. In the case of small curvature ($h_0 M_0 < 1$), the spontaneous curvature is:

$$M_0 = k_B T N^2 \Gamma^{(2+\nu)/2\nu} / 8\nu b \kappa \quad (3)$$

in which $\Gamma = b^2/S$ (S is the cross-sectional area of the FPOSS). It scales as $M_0 \sim N^2 \Gamma^{13/6} \kappa^{-1}$ in the case of self-avoiding chains ($\nu = 3/5$).[12d] The estimated values of the spontaneous curvatures are listed in Table 1 (see the Supporting Information). Because the curvature formation is a spontaneous process, M_0 is an upper limit of the accessible curvature. It thus provides a direct comparison between calculations (M_0) and experimental observations (M_{max}; Table 1). According to Equation (3), the M_{max} value increases with increasing tail length, and decreases with increasing tethering-point distance and bending rigidity. The tail-length effect could be confirmed by comparing the concentric lamellae formed by giant surfactants with the same architecture but different tail lengths (see Figures S3 and S4). For the linear giant surfactants (FPOSS-PS and FPOSS-PS-*b*-PEO), a larger M_{max} value is observed for FPOSS-PS when both have a similar overall degree of polymerization, which could be attributed to the reduced monomer size of PEO ($b = 0.50$ nm) as compared to PS ($b = 0.68$ nm).[15] The M_{max} value also depends on the molecular architecture. For the giant surfactants with block-copolymer tails (FPOSS-PS-*b*-PEO and PS-(FPOSS)-PEO), the linear surfactant usually has larger curvature than the starlike surfactant, probably as a result of different molecular packing. The PEO and PS blocks in the lamellae formed by PS-(FPOSS)-PEO occupy different sections of the polymer domain, which reduces chain overcrowding.[9]

Thermodynamically, although the formation of the initial curved nuclei is more energetically favorable than the formation of flat nuclei ($\Delta F = -0.56\, k_B T$ per molecule; see the Supporting Information), the growth of the lamellae on the curved nuclei has to overcome a higher energy barrier (Figure 3). During growth, the molecules depositing on the curved nuclei adopt an opposite curvature, which leads to even more severe excluded-volume repulsion of the polymer tails. However, as compared with the disordered mixture, the molecules in the oppositely curved layers still possess a lower free energy, and the deposition process is energetically favorable. Further growth on this oppositely curved layer leads to the formation of a bilayer with symmetric molecular packing, which in principle prefers flat interfaces. Taking FPOSS-PS as an example, a lamellar bilayer (PS/FPOSS// FPOSS/PS) consists of two monolayers (FPOSS/PS) with opposite curvatures (see Scheme S1). Upon bending, the entropy gain of the polymer chain on the convex side offsets the entropy loss on the corresponding concave side.[12d] According to Equation (1), the entropy contribution disappears and the bending energy determines the overall free-energy change of the bilayer, $\Delta F = \Delta F_b(M) = 1/2\kappa\xi_0^2 M^2$, which could be modified to relate the bending modulus to the molecular parameters [see Eq. (S4) in the Supporting Information].[12a–c] A typical bending energy is estimated to be around $0.01\, k_B T$ per chain, which is relatively small as compared with the energy gain of the initial monolayer.[1c,7b] Moreover, the curvature of the curved bilayers gradually decreases with increasing radius along the radial direction, which further diminishes the bending energy. The bending energy during growth is accumulative, and beyond a critical size, the total energy cost will exceed the energy gain of the formation of the initial monolayer. This effect might partially be the reason why the size of concentric lamellae cannot spread to infinity. Below the critical size, the curved/concentric lamellae possess a lower free energy as compared to the flat lamellae and thus are thermodynamically more stable, which provides the driving force for their spontaneous formation. The population of the curved/concentric lamellae and the flat lamellae depends on both the nucleation and growth processes. An increase in the molecular weight of the polymer tail(s) will lead to an increased population of curved/concentric lamellae. A compromise between thermodynamics (preferential formation of curved nuclei) and kinetics (preferential growth on the flat nuclei) leads to the coexistence of flat and curved lamellae.

In summary, curved/concentric lamellae with smooth curvatures were observed in FPOSS-based giant surfactants. The FPOSS provides a rectangular molecular interface between the FPOSS head and polymer tail(s). The chain overcrowding of polymer tails generates a truncated-wedge-like molecule shape. The nucleation and growth process during phase separation leads to the formation of curved and concentric lamellae. Curved/concentric lamellae were observed in giant surfactants with different architectures and compositions, thus confirming the generality of our hypothesis. Such spontaneous curvature formation may provide a promising and efficient path toward the fabrication of a wide range of high-performance devices.

Acknowledgements

This research was supported by the National Science Foundation (DMR-1409972).

Keywords: concentric lamellae · curvature · giant surfactants · polymers · self-assembly

How to cite: *Angew. Chem. Int. Ed.* **2016**, *55*, 2459–2463
Angew. Chem. **2016**, *128*, 2505–2509

[1] a) E. Saitoh, H. Miyajima, T. Yamaoka, G. Tatara, *Nature* **2004**, *432*, 203–206; b) F. J. Castano, D. Morecroft, W. Jung, C. A. Ross, *Phys. Rev. Lett.* **2005**, *95*, 137201; c) Y. S. Jung, W. Jung, C. A. Ross, *Nano Lett.* **2008**, *8*, 2975–2981.

[2] a) F. S. Bates, *Science* **1991**, *251*, 898–905; b) F. S. Bates, M. A. Hillmyer, T. P. Lodge, C. M. Bates, K. T. Delaney, G. H. Fredrickson, *Science* **2012**, *336*, 434–440.

[3] M. Ma, K. Titievsky, E. L. Thomas, G. C. Rutledge, *Nano Lett.* **2009**, *9*, 1678–1683.

[4] F. S. Bates, G. H. Fredrickson, *Annu. Rev. Phys. Chem.* **1990**, *41*, 525–557.

[5] a) X. He, M. Song, H. Liang, C. Pan, *J. Chem. Phys.* **2001**, *114*, 10510–10513; b) G. J. A. Sevink, A. V. Zvelindovsky, J. G. E. M. Fraaije, H. P. Huinink, *J. Chem. Phys.* **2001**, *115*, 8226–8230; c) A.-C. Shi, B. Li, *Soft Matter* **2013**, *9*, 1398–1413.

[6] a) S. Koizumi, H. Hasegawa, T. Hashimoto, *Macromolecules* **1994**, *27*, 6532–6540; b) K. Shin, H. Xiang, S. I. Moon, T. Kim, T. J. McCarthy, T. P. Russell, *Science* **2004**, *306*, 76; c) Y. Wu, G. Cheng, K. Katsov, S. W. Sides, J. Wang, J. Tang, G. H. Fredrickson, M. Moskovits, G. D. Stucky, *Nat. Mater.* **2004**, *3*, 816–822; d) M. Ma, V. Krikorian, J. H. Yu, E. L. Thomas, G. C. Rutledge, *Nano Lett.* **2006**, *6*, 2969–2972; e) P. Dobriyal, H. Xiang, M. Kazuyuki, J.-T. Chen, H. Jinnai, T. P. Russell, *Macromolecules* **2009**, *42*, 9082–9088.

[7] a) J. Y. Cheng, C. T. Rettner, D. P. Sanders, H.-C. Kim, W. D. Hinsberg, *Adv. Mater.* **2008**, *20*, 3155–3158; b) G. M. Wilmes, D. A. Durkee, N. P. Balsara, J. A. Liddle, *Macromolecules* **2006**, *39*, 2435–2437; c) J. Chai, D. Wang, X. Fan, J. M. Buriak, *Nat. Nanotechnol.* **2007**, *2*, 500–506.

[8] B. Ni, X.-H. Dong, Z. Chen, Z. Lin, Y. Li, M. Huang, Q. Fu, S. Z. D. Cheng, W.-B. Zhang, *Polym. Chem.* **2014**, *5*, 3588–3597.

[9] X.-H. Dong, B. Ni, M. Huang, C.-H. Hsu, Z. Chen, Z. Lin, W.-B. Zhang, A.-C. Shi, S. Z. D. Cheng, *Macromolecules* **2015**, *48*, 7172–7179.

[10] a) B. Ni, M. Huang, Z. Chen, Y. Chen, C. H. Hsu, Y. Li, D. Pochan, W. B. Zhang, S. Z. D. Cheng, X. H. Dong, *J. Am. Chem. Soc.* **2015**, *137*, 1392–1395; b) J. He, K. Yue, Y. Liu, X. Yu, P. Ni, K. A. Cavicchi, R. P. Quirk, E.-Q. Chen, S. Z. D. Cheng, W.-B. Zhang, *Polym. Chem.* **2012**, *3*, 2112–2120.

[11] T. Hashimoto, N. Sakamoto, *Macromolecules* **1995**, *28*, 4779–4781.

[12] a) S. T. Milner, T. A. Witten, *J. Phys. Fr.* **1988**, *49*, 1951–1962; b) Z.-G. Wang, S. A. Safran, *J. Chem. Phys.* **1991**, *94*, 679–687; c) Z.-G. Wang, *J. Chem. Phys.* **1994**, *100*, 2298–2309; d) C. Hiergeist, R. Lipowsky, *J. Phys. IV* **1996**, *6*, 1465–1481.

[13] W. Helfrich, *Z. Naturforsch. C* **1973**, *28*, 693–703.

[14] a) S. Alexander, *J. Phys.* **1977**, *38*, 983–987; b) P. G. de Gennes, *Macromolecules* **1980**, *13*, 1069–1075; c) R. Cantor, *Macromolecules* **1981**, *14*, 1186–1193; d) P. J. Flory, *Principle of Polymer Chemistry*, Cornell University Press, Ithaca, **1981**; e) M. Rubinstein, R. H. Colby, *Polymer Physics*, Oxford University Press, Oxford, **2004**.

[15] L. Zhu, S. Z. D. Cheng, B. H. Calhoun, Q. Ge, R. P. Quirk, E. L. Thomas, B. S. Hsiao, F. Yeh, B. Lotz, *Polymer* **2001**, *42*, 5829–5839.

Received: November 12, 2015
Published online: January 15, 2016

